

ANALYSIS OF HORIZONTAL CLOSED ORBITS VS FREQUENCY

S. van der Meer

1. Introduction

Inspection of the horizontal closed orbit shape at different revolution frequencies (i.e. energies) shows that at frequencies far away from the central one the orbits present large asymmetries with respect to the two symmetry axes of the machine. This reduces the aperture near the stack bottom by about 11 mm. In addition, the aperture available for the injected beam is about 2 mm smaller than for a beam at the central frequency because of orbit deformations in the long straight sections (LSS).

The asymmetries were more pronounced in the past. A certain amount of improvement was obtained during 1981 by connecting different shunts across the individual QFW quadrupoles. However, it seemed clear from the outset that these quads themselves could not be the reason for the asymmetries observed and that it would be preferable to correct the field errors at the source. Because the vertical orbits are much better than the horizontal ones, it seems clear that the source must be found in the bending magnets and their stray fields, or perhaps in the influence of the ferrites in the cooling tanks on the quadrupole stray fields.

Although the orbit distortions do not lead to catastrophic losses, it still seems interesting to correct them. With this in mind, I tried to find the causes for the asymmetries. The conclusion is that the largest contribution must be from differences in field distribution between the four BLG ends away from the LSS. The discrepancies are so large that correction would be quite difficult.

2. Data Used

The analysis is based upon measurements of closed orbits on 15th May, 1981, 11th November 1981, 22nd December 1981, 11th May 1982 and 6th June 1982 (at the last date, both the p and \bar{p}). The 1982 data are probably the most

reliable, mainly because after the recent shielding improvements higher circulating beam intensities were used.

3. Subtraction of Central Orbit

We shall only consider orbit variations with frequency, disregarding any orbit deformations that do not depend on frequency and that may be corrected in the usual way (e.g. by displacing quadrupoles). Thus, we subtract the central orbit from all other ones. The orbits then represent what would be left if the central orbit would be straightened out perfectly by classical means. All orbit bumps created for special purposes also disappear.

4. Asymmetries at the F1 quads

In the high-dispersion regions of the lattice (i.e. away from the LSS) there are two types of F quadrupoles, called F1 and F2 (see Fig. 1). The asymmetry at the F1 quads is the easiest to understand.

To this end, we calculate for different frequencies at what radial position a particle would arrive at the first F1 quad if it would start out along the centre line in the LSS. This can be derived from the measured closed orbit by displacing and tilting it in the LSS until it coincides with the centre line and then applying the corresponding corrections to the measured positions in the F1 quads (see Fig. 2).

In practice, we find that these corrections are small (<2 mm) and that the observed asymmetry persists. The important point, however, is that after this treatment the remaining asymmetry is completely decoupled from what happens anywhere else in the ring. It can now only come from field errors between the LSS and the F1 quads; the individual quadrupole shunts, the BST's and the ferrite effects are excluded. In fact, since we consider differences with respect to the central orbit, the only field errors that can contribute are those in regions with non-zero dispersion. The only important remaining error sources are the BLG ends near the QD quads (away from the LSS).

The displacements with frequency at the F1 quads are quite large (± 230 mm). To appreciate the asymmetries, we subtract the average position from the measurements, so that the deviations stand out clearly. Since we

do not know the theoretical position vs frequency with sufficient precision, we subtract (somewhat arbitrarily) the following amount:

$$x = -43.04 \Delta f - .6228 \Delta f^2 \quad (1)$$

with $\Delta f = f - 1850.37$ (x in mm, f in kHz).

This gives a reasonable empirical fit to the most recent measurements. The resulting deviations are plotted in Figs. 3-5 for the different measurements. Note that the average shape depends on the arbitrary assumption (1) but that the differences between the four F1 curves are what concerns us here.

5. Discussion of the F1 Asymmetry

Inspection of Figs. 3-5 shows the following facts:

- a) For the oldest measurements (22nd December 1981 and before) we see a general slope of the curves. This is caused by the lower Q_H value at that time, resulting in a lower γ_T , a larger $|\eta|$ and therefore a smaller $\Delta p/p$ for the same frequency difference. The order of magnitude of the slope agrees with this explanation.
- b) The measurement at QFW 22 seems to be completely different on 11th May 1982 for no clear reason. The only explanation seems to be that something went wrong with the pick-up calibration.
- 3) Considering the last 3 measurements (which are the most reliable) we notice differences between the four F1's that persist. The most conspicuous is the different shape of the QFW 4 curve (which could be caused by a sextupole-type error at the end of BLG2), but the average slope of the curves, corresponding to quadrupole-type errors, is also different.

6. Possible Causes

It is easy to calculate what field errors are needed to explain the observed effects, and the results are astonishing. For instance, to explain the difference in slope at QFW10 vs QFW16 or 22 on 4th June 1982 (Fig. 3), we would require an error of integrated gradient at the end of BLG11 equivalent to 7% of the strength of QDN 11. For explaining the curvature at QFW4, field errors of a similar magnitude are needed.

To remove the asymmetry at QFW4, the deflection at the end of BLG2 would have to be 0.4 mr larger at the extreme frequencies than at the centre frequency. This would necessitate an increase of effective length of 3 mm at the extreme frequencies, requiring shims of 6 mm thickness. However, the α_p value at the BLG end is relatively low, so that the beam position varies by only 10 cm over the entire frequency range. The aperture is larger than this (because of horizontal emittance) and the shim thickness would certainly have to be much larger further outside.

The measurements made on the BLG's before installation in the ring predict effective length variations that are small compared to 3 mm over the central 10 cm of the aperture (at least 10 times less). However, it seems impossible to find any other cause for the asymmetry. For instance, remanent field errors of the injection kicker would have to be enormous because it is near QFW4. Any stray field variations in the empty part of straight section 3 are certainly at least an order of magnitude less than needed to explain the effects. Also for the other F1's, the BLG ends seem to be the only possible culprits.

It would be tempting to ascribe the effects to errors in the individual pick-up measurements. However, not only are the errors supposed to be much smaller than this¹⁾, but we can see from similar curves calculated for the F2 positions (Fig. 6-7) that the extra curvature at QFW6 is very similar to the one at QFW4. Although the F2 positions depend on many more parameters than those at the F1's (e.g. F1 shunts, ferrites, BST errors), the correlation seems clear and it is difficult to believe that the pick-ups at QFW4 and QFW6 produce the same effects by accident.

7. Orbit Errors vs Frequency in the LSS

Fig. 8 shows the orbits in the LSS, again after subtracting the central orbit. In this case, the absolute values rather than the differences between the four curves are important.

At pick-ups 2 and 14 the same curvature as noted before at QFW4 appears. Most of this curvature would disappear if the end of BLG2 were corrected as described above. This again confirms the reality of the effect.

Note that the slope of these curves (as well as for the QFW curves) might be corrected by adjusting the shunts across the QFW's, even though

1) G. Gelato, H. Koziol, M. Le Gras, D.J. Williams, The closed Orbit Observation System of the CERN Antiproton Accumulator, IEEE Trans. Nucl. Sci., NS-28, June 1981, p-2186

this would probably not attack the errors at the source.

8. Correction by Shimming

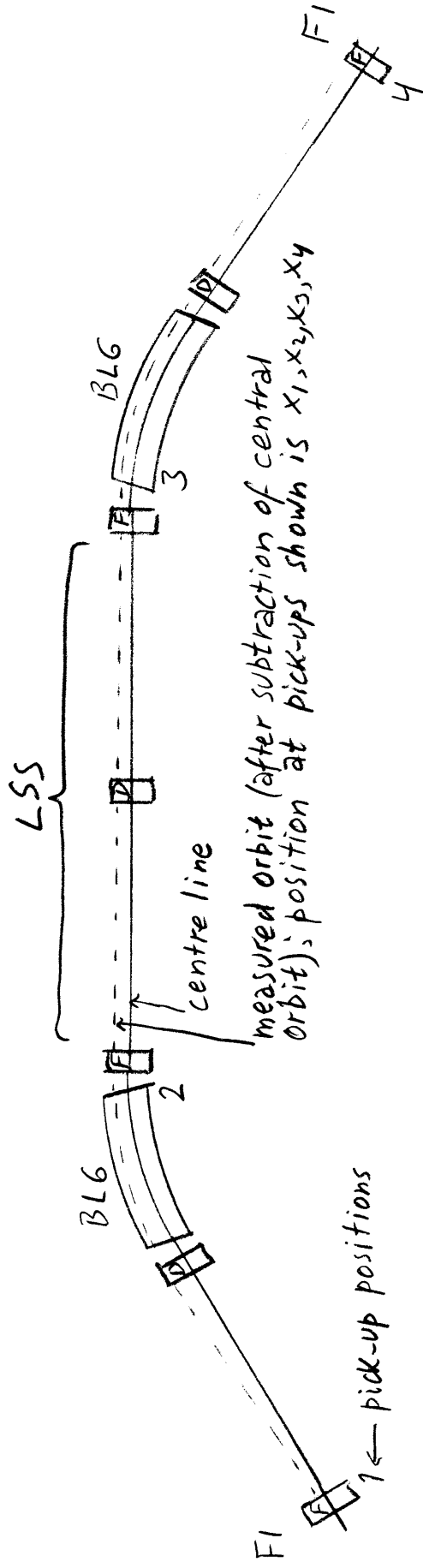
If we would try to correct the curvature at QFW4 by shimming the end of BLG2 alone, we would introduce an intolerable sextupole error; the resulting ΔQ_y between the extreme frequencies would be about 0.15. We would therefore have to make opposite, smaller, corrections on the other BLG ends or elsewhere, to compensate for this, remembering that it is only the difference between the four curves that counts.

However, we would have to do additional shimming on some of the BST's to obtain acceptable closed orbits after the BLG changes. Calculation shows that these would be of the same order of magnitude as on the BLG's.

It is possible to find the required changes in integrated field with good precision. However, the exact shim thicknesses needed are not known sufficiently well. Especially for the BLG's, which have a vertical aperture comparable to the horizontal width across which the changes are needed, the results cannot be predicted with confidence. As a result, after such a shimming exercise, the asymmetries (calculated as outlined above) would probably be much smaller but a second and third round of shimming might well be needed to obtain acceptable orbits and Q values.

9. Conclusion

Even if we believe the results of the closed orbit measurements despite the contradiction with the original BLG field measurements, the possible gain in aperture does not seem large enough to justify reshimming. This operation would in any case be quite difficult because of the poor accessibility of the BLG and BST ends.



For an orbit starting out with $x_2^* = x_3^* = 0$, we would have

$$x_1^* = x_1 + C(x_2 \sin(\mu_1 - \mu_3) - x_3 \sin(\mu_1 - \mu_2))$$

$$x_4^* = x_4 + C(x_2 \sin(\mu_4 - \mu_3) - x_3 \sin(\mu_4 - \mu_2))$$

$$\text{with } C = \frac{\sqrt{\beta_1 / \beta_2}}{\sin(\mu_3 - \mu_2)}$$

Fig. 2. Calculating the F1 positions for a particle starting out on the centre line in a LSS.

4-6-82

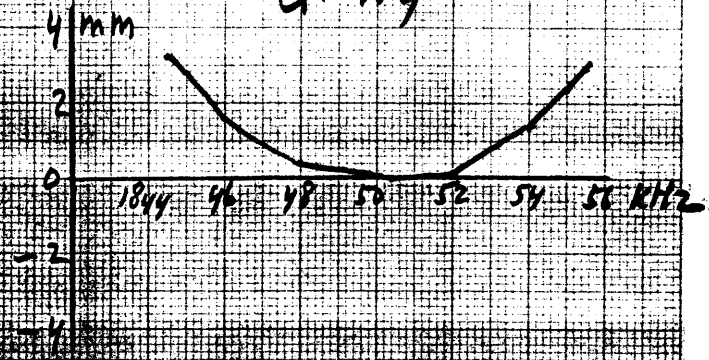
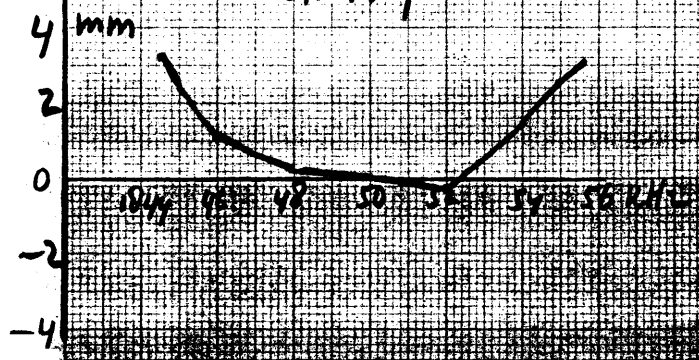
4-6-82

P

P

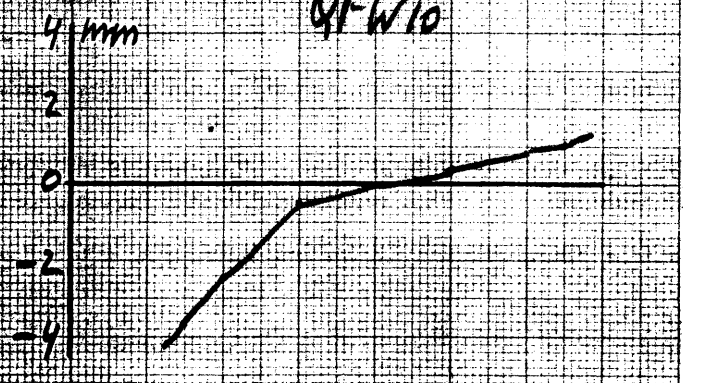
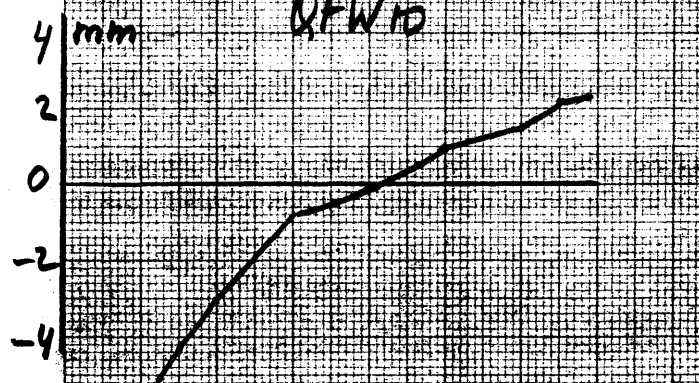
QFW4

QFW4



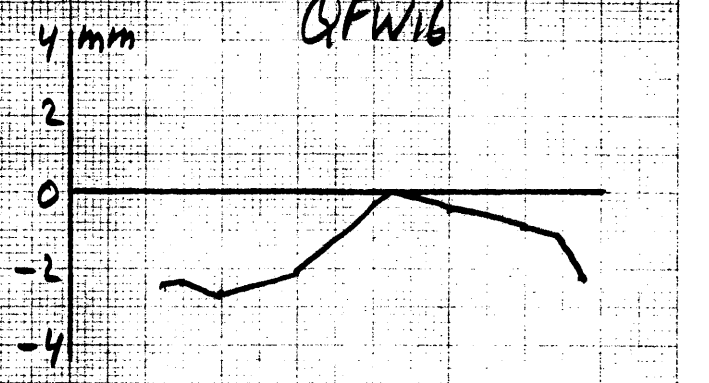
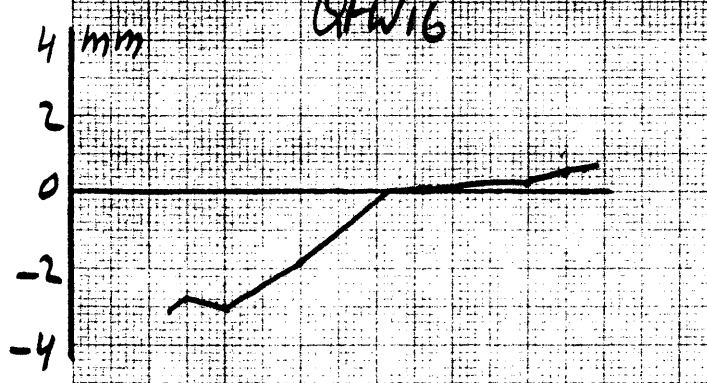
QFW10

QFW10



QFW16

QFW16



QFW22

QFW22

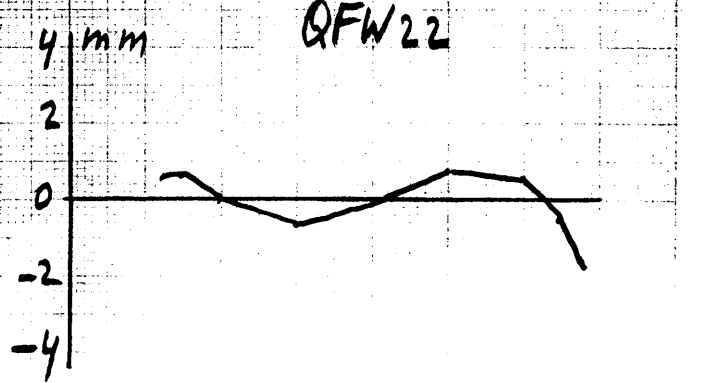
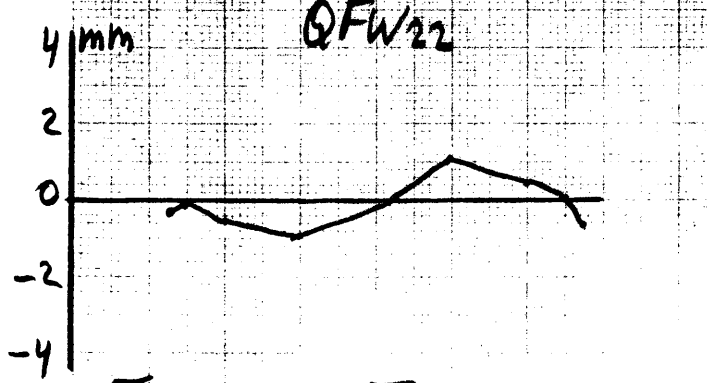


Fig. 3 F1 asymmetries

11-5-82

22-12-81

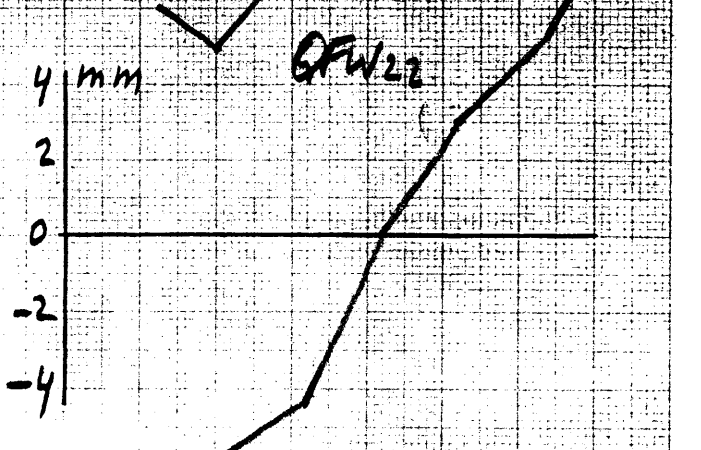
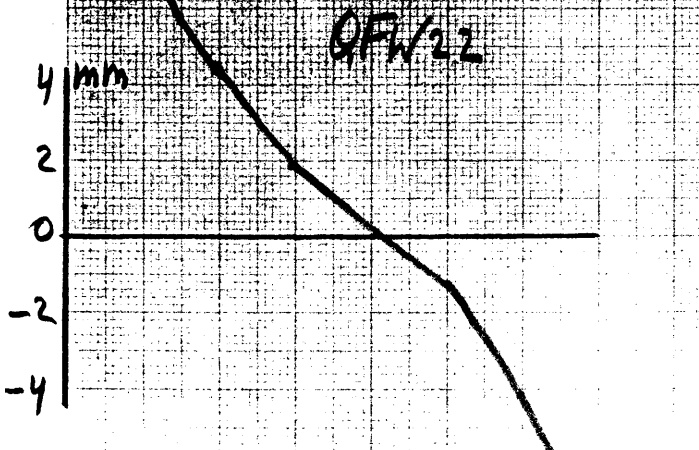
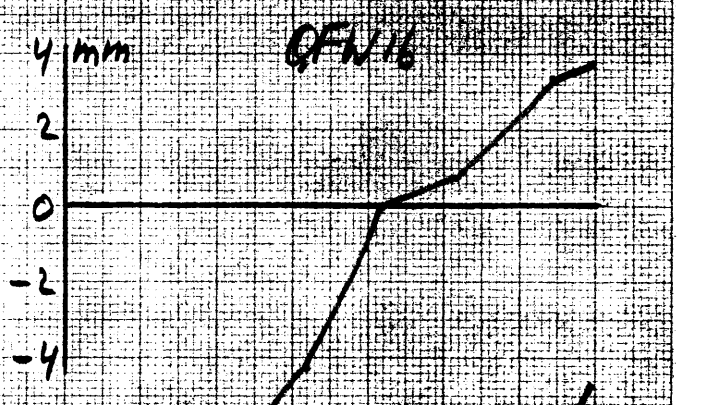
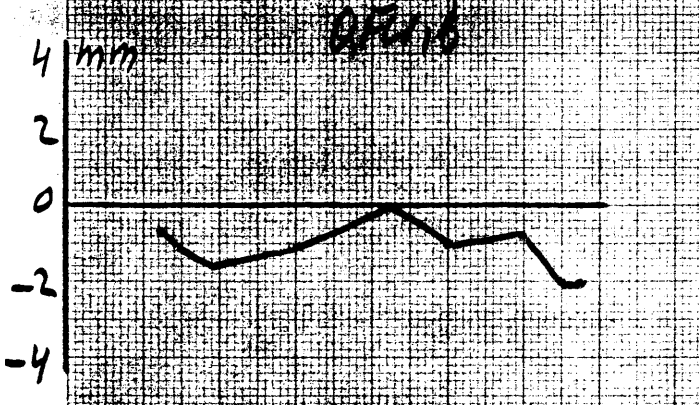
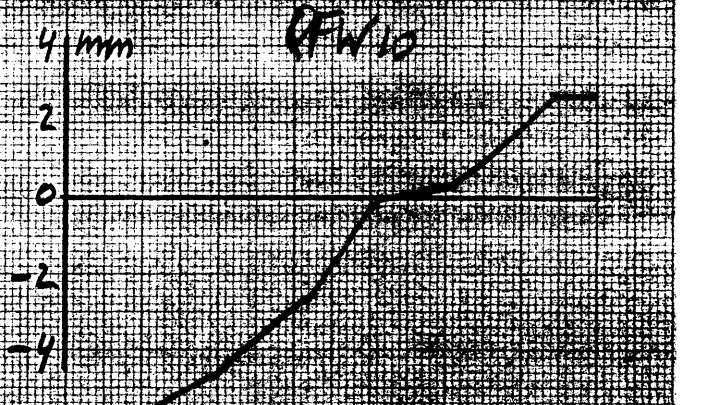
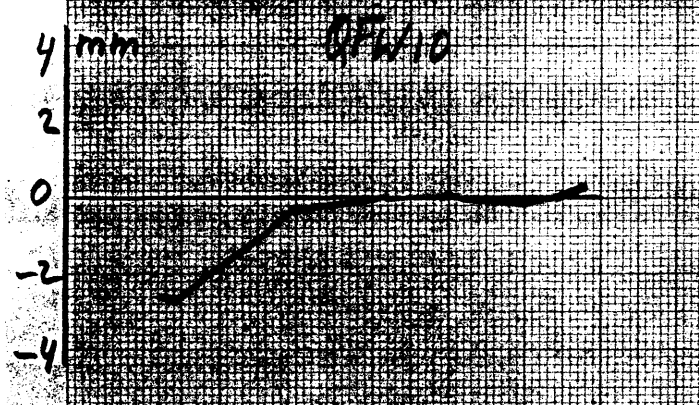
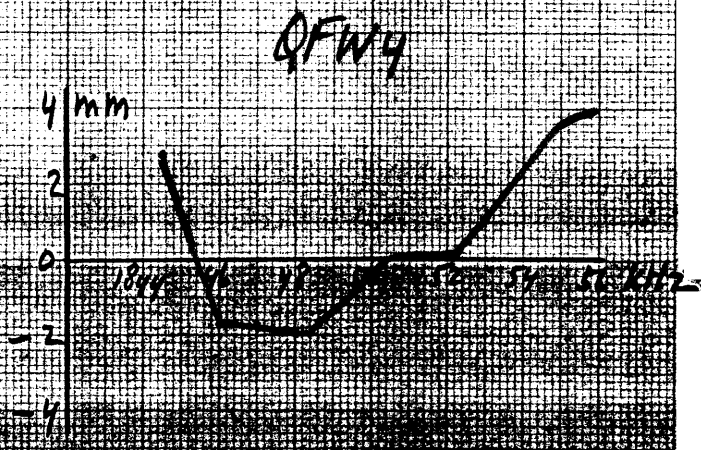


Fig. 4 - Fl asymmetries

11-11-81

15-5-81

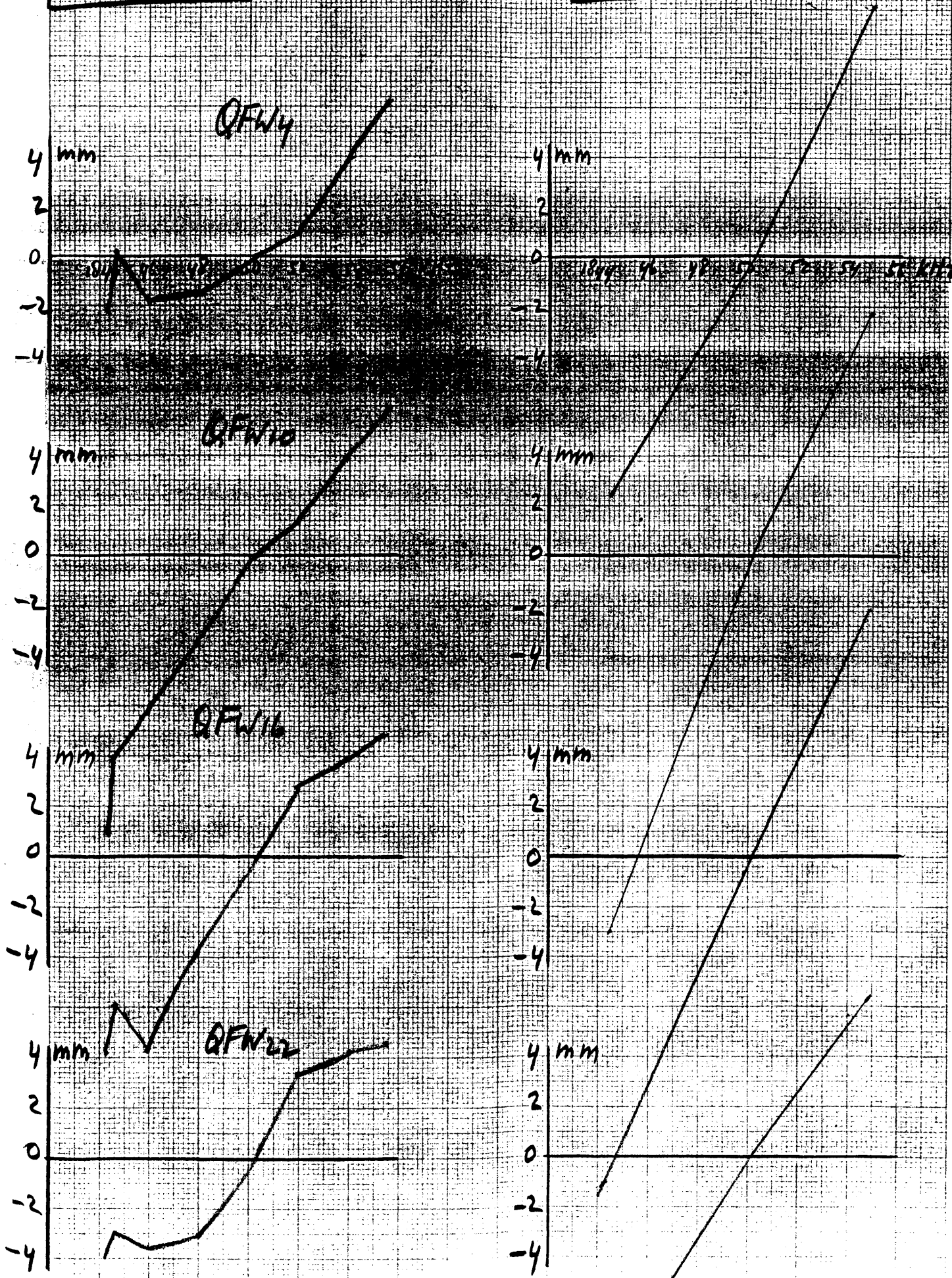


Fig. 5 F1 asymmetries

4-6-82

P

4-6-82

P

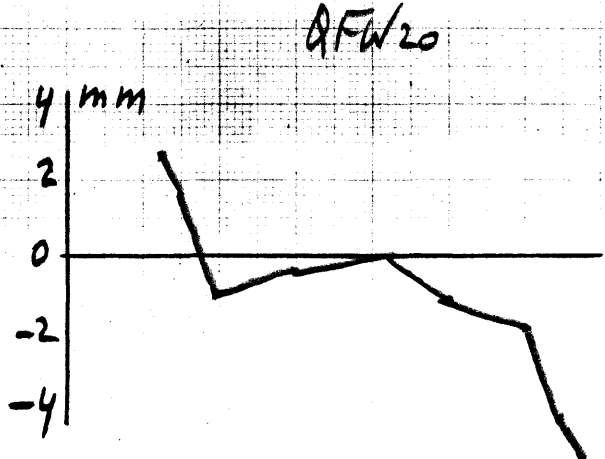
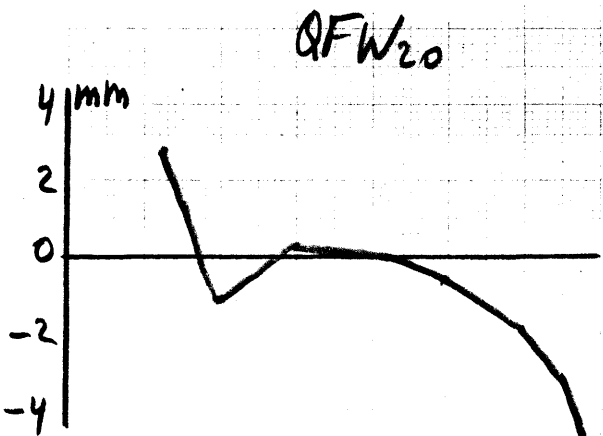
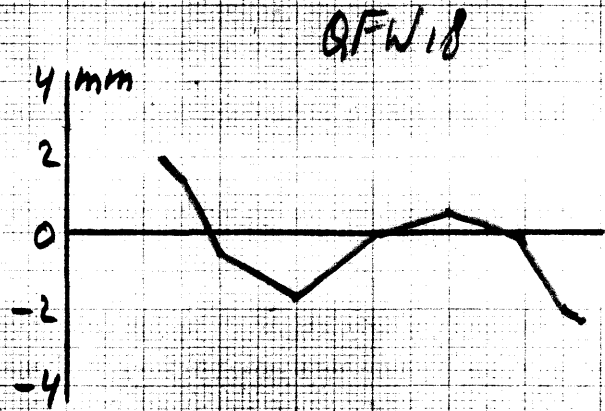
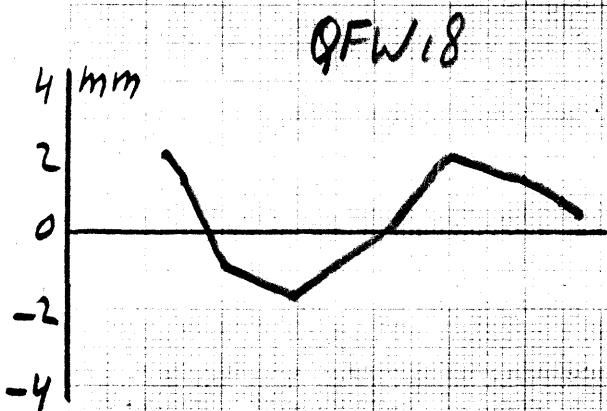
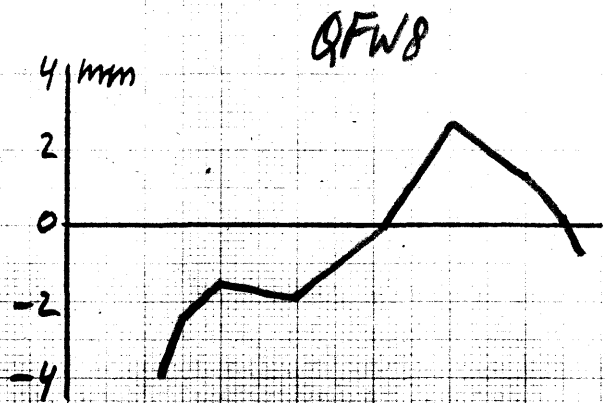
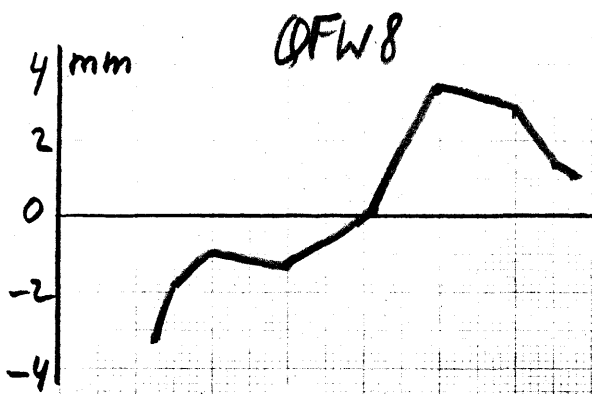
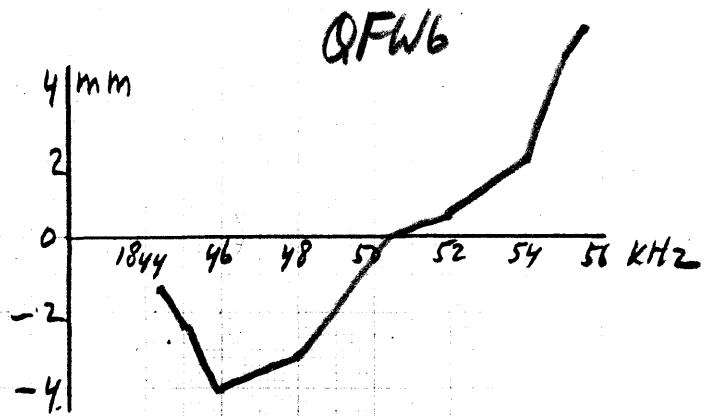
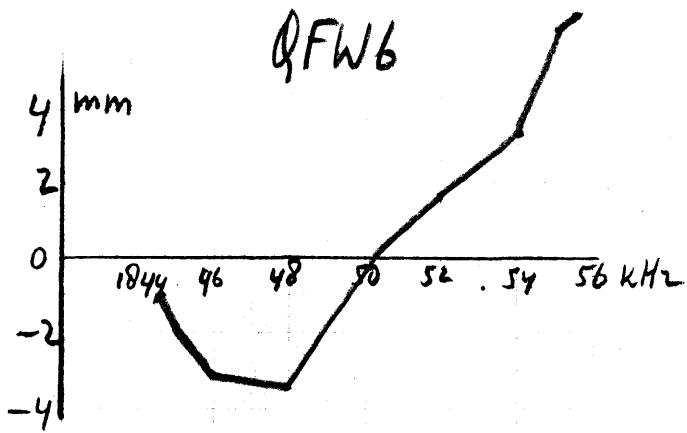


Fig.6 F2 asymmetries

11-5-82

22-12-81

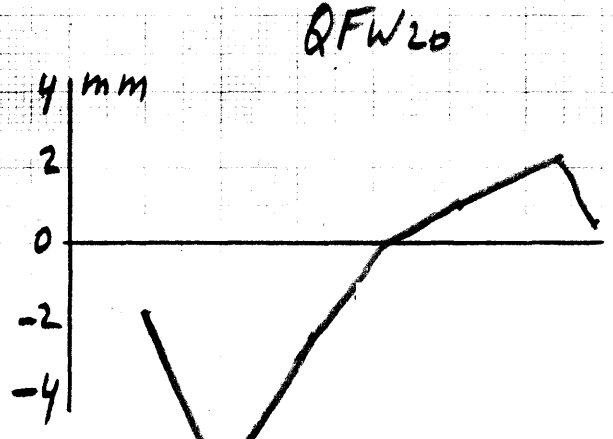
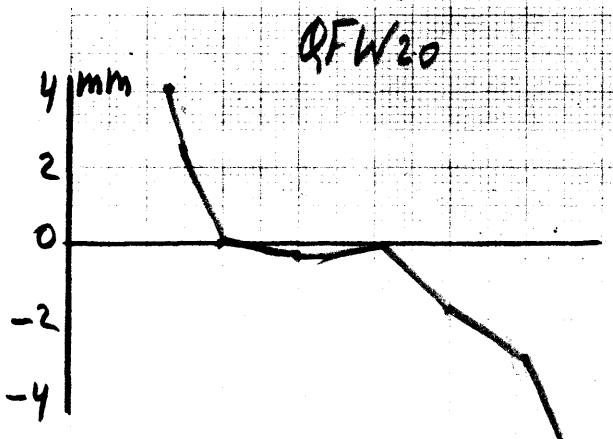
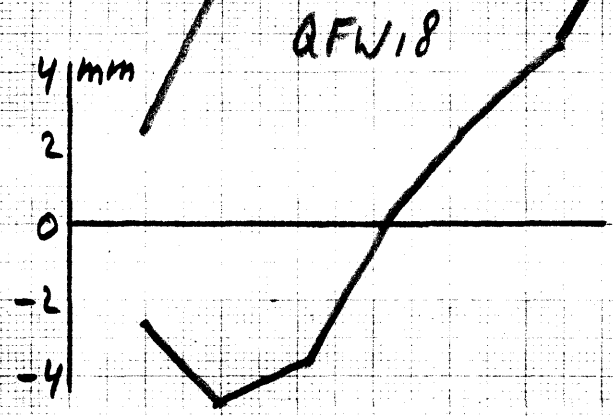
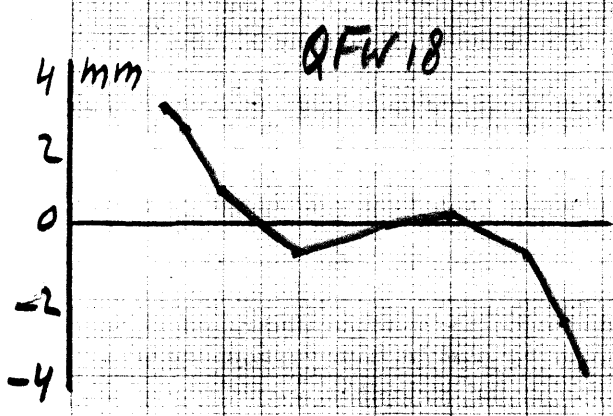
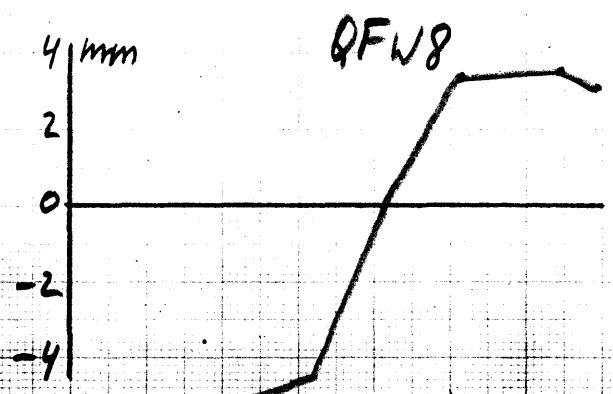
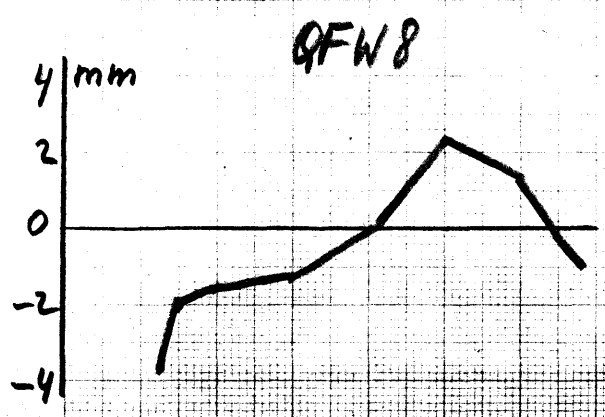
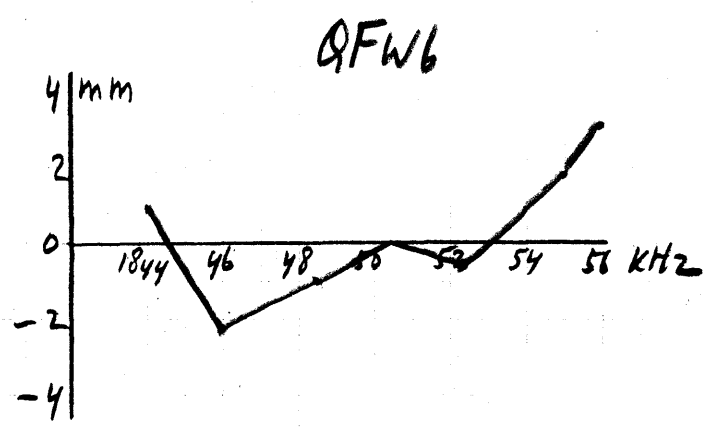
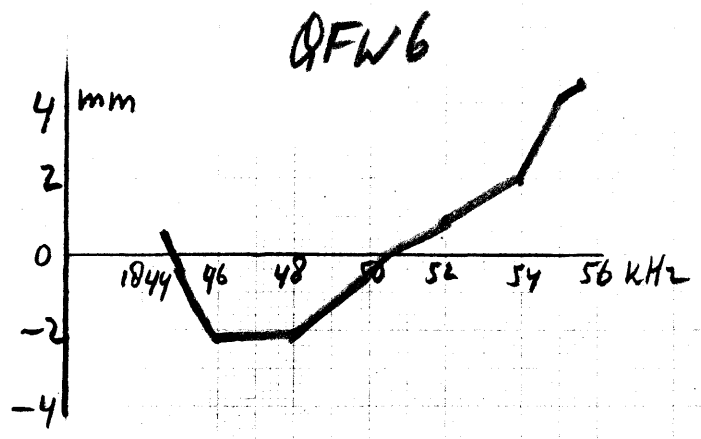
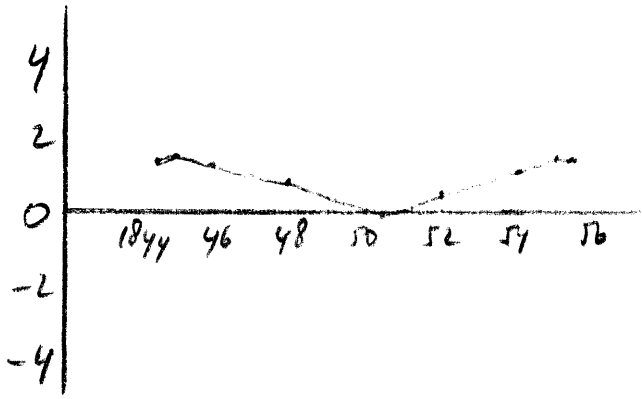
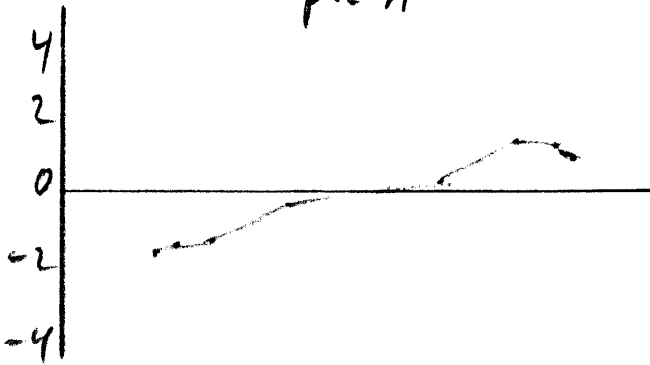


Fig. 7. F2 asymmetries

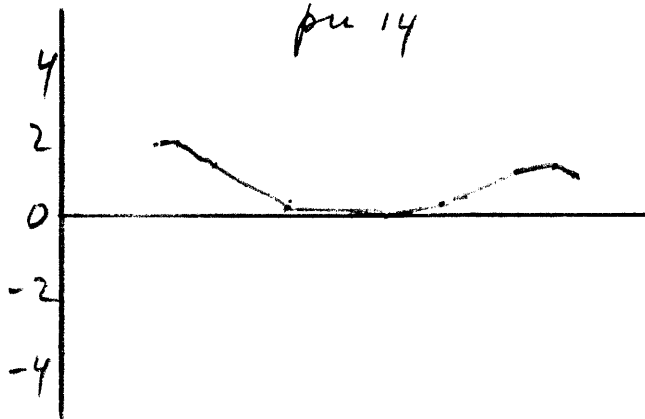
pu 2



pu 11



pu 14



pu 23

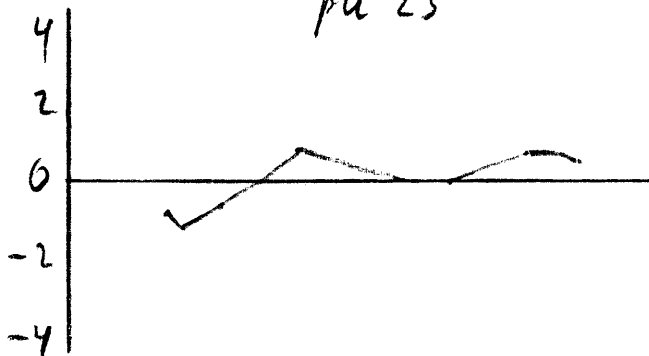


Fig. 8 LSS orbits